International Journal of Nanomedicine

Dovepress
open access to scientific and medical research

Open Access Full Text Article

ORIGINAL RESEARCH

# Microneedle Patch Delivery of Methotrexate-Loaded Albumin Nanoparticles to Immune Cells Achieves a Potent Antipsoriatic Effect

Huaiji Wang[1,*], Zihan Zhao[2,*], Chenghao Wu[3,*], Xiaowen Tong[3], Yuling Shi[2], Shunjie Chen[1]

[1]Department of Nephrology, Shanghai Fourth People's Hospital, School of Medicine, Tongji University, Shanghai, People's Republic of China; [2]Department of Dermatology, Shanghai Skin Disease Hospital, Tongji University School of Medicine, Shanghai, 200443, People's Republic of China; [3]Department of Obstetrics and Gynecology, Tongji Hospital, Tongji University School of Medicine, Shanghai, 200065, People's Republic of China

*These authors contributed equally to this work

Correspondence: Shunjie Chen, Department of Nephrology, Shanghai Fourth People's Hospital, School of Medicine, Tongji University, Shanghai, People's Republic of China, Email chenshunjie77csj@163.com



**Introduction:** Transdermal drug delivery provides a desirable alternative method of penetrating the skin for psoriasis treatment, by virtue of its ability to dampen the overactivation of immune cells and inflammation, while attenuating the detrimental effects of systemic administration. Lymph nodes (LNs), as a critical organ of the lymphatic and the acquired immune system, are suitable sites for drug homing to suppress the immune cells.

**Methods:** In this context, we developed a microneedle (MN) patch that delivers nanodrugs locally to LNs for improving the antipsoriatic treatment. In this study, human serum albumin nanoparticles carrying methotrexate (HM) were synthesized and loaded into hyaluronic acid (HA)-based microneedles (HM/MN).

**Results:** The patch showed an excellent ability to pierce the skin, which enhanced drug delivery. In a mouse model of psoriasis, the HM/MN patch significantly prevented the erythema with decreased skin thickness, thus inhibiting the progression of psoriasis. Further analysis for immune cells in LNs, the percent of dendritic cells (DC) and T cells reduced after the local treatment with HM/MN. Notably, the feasibility of targeted delivery of methotrexate to LNs using nanoparticles was verified by detecting increased accumulation of methotrexate in LNs. In addition, the HM/MN patch pronouncedly decreased the levels of tumor necrosis factor α and interleukin 6 in the skin.

**Conclusion:** The results suggested the high efficacy of using the HM/MN patch to treat psoriasis, and provided new insight into the mechanism of the transdermal drug delivery system.

**Keywords:** microneedles, transdermal drug delivery, psoriasis, lymph node homing, nanodrug

## Introduction

Psoriasis is an incurable chronic inflammatory autoimmune disease with a high recurrence rate that affects the skin, joints and nails, and whose main pathological mechanisms include immune imbalance and damaged skin barrier.[1] The etiology of psoriasis is complex, and involves T cell activation, inflammatory cell infiltration, keratinocyte hyperproliferation, etc.[2]

With the advances in the understanding of the immune mechanism underlying the pathogenesis of psoriasis, therapeutics aimed at regulating the immune response have been gradually introduced for the clinical treatment of psoriasis. Methotrexate (MTX), an affordable small molecule immunosuppressant drug, can suppress the immune system, and is considered the first-line systemic drug for treating most moderate-to-severe psoriasis.[3,4] However, traditional oral administration usually leads to adverse effects, such as oral ulcers, gastrointestinal intolerance, myelosuppression and toxicity to the liver and lung. Approximately 30% of patients were discontinued from MTX treatment due to liver toxicity and lack of effective measurement to precisely predict the therapy outcome and side effects in the clinic, creating a dilemma for its wide application.[5,6]

Received: 22 April 2022
Accepted: 2 August 2022
Published: 1 September 2022

A transdermal drug delivery system for local treatment could target the diseased region of the skin, and is considered as an effective approach for the management of psoriasis, that reduces the adverse effects due to systemic administration.[7–10] However, the stratum corneum, the outermost lipophilic and dead layer of skin that acts as a first barrier to foreign substances entering the body, water leaving the body, and drug delivery, limits the transdermal penetration efficiency and reduces the bioavailability of the drug.[11] Remarkably, MN can directly pierce the stratum corneum, greatly promoting the efficiency of transdermal drug delivery.[12,13] Therefore, MN patches have been widely applied in the treatment of superficial tumors, scars, psoriasis, herpes, acne and hair loss.[14] Soluble MN have the hallmarks of a simple preparation process, low cost, large drug loading, and no needle tip waste after application, and have thus attracted considerable interest.[15] Soluble MN are arrays of micron-sized needles, which form reversible microchannels on the skin surface by piercing the stratum corneum and increasing the penetration of drugs, thereby improving the transdermal absorption of therapeutic agents. As a minimally invasive drug delivery system, the MN are long enough to pierce the stratum corneum, but not so short and thin to touch the pain nerves in the deep layers of the skin, thus avoiding pain.

Hyaluronic acid (HA), a biocompatible polysaccharide that is ubiquitously present in connective, epithelial, and neural tissues, body fluids and skin, is widely used in skin care cosmetics and injectable soft tissue fillers. Therefore, its high biocompatibility and clinical safety make HA an excellent candidate material for the preparation of soluble MN.[16,17] In addition, advances in nanotechnology can further improve the efficiency of drug delivery with higher loading and responsive release.[18,19] Among drug carriers, human serum albumin (HSA) nanoparticles (NP), according to the previous report, are biocompatible and can target LNs, which can effectively improve the delivery of MTX to the LNs to inhibit the activation of immune cells.[20–22]

Accordingly, in this study, we constructed an innovative transdermal drug delivery system by filling a HA-based MN patch with MTX-loaded HSA NP to obtain HSA NP carrying MTX (HM) loaded into the HA-based MN patch (hereafter referred to as HM/MN patch). The HM/MN patch consisted of 15×15 needle assays, distributed on the base of 1–2 $cm^2$. The size of each needle was about 180 μm × 180 μm × 550 μm, with a needle space of 500 μm. The HSA NP were loaded into the soluble MN through two-step casting, which not only ensured high-load efficiency, but also enabled the achievement of sufficient mechanical strength to deliver drugs through the skin, thereby increasing the efficiency of the transdermal delivery system. The soluble MN allowed the delivery of micro-scale volumes of drugs into the body, with decreased drug loss, sustained drug release capability and targeted delivery to LNs tissues. In this study, we aimed to deliver MTX nanodrug through a MN patch to investigate its regulatory effect on the immune system in a mouse model of psoriasis. The patch solved the problems of transdermal precise administration and sustained drug release, and greatly reduced the side effects of the traditional MTX treatment, making it a feasible treatment for psoriasis.

# Materials and Methods

## Materials

Human serum albumin (HSA), 2-(N-Morpholino) ethanesulfonic acid (MES), fluorescein isothiocyanate (FITC) were purchased from Sigma-Aldrich (Shanghai) Trading Co., Ltd. MTX (≥98%), sodium dodecyl sulfate (SDS, ≥98%), dimethylsulfoxide (DMSO, ≥99%) were obtained from Shanghai Aladdin Biochemical Technology Co., Ltd. Sodium hyaluronate (5 kDa) was purchased from Bloomage Freda Biopharm Co., Ltd., (Jinan, China). Paraformaldehyde (4%) was obtained from Beyotime Biotechnology Co., Ltd. Imiquimod cream (5%) was from Mingxin Pharmaceuticals (Sichuan, China). CD16/32, APC-Cy7-CD45, FITC-CD3, Qdot-605-CD11c were bought from BioLegend Inc. RPMI 1640 medium and fetal bovine serum (FBS) were purchased from Thermo Fisher Scientific Inc.

## Characterization

UV-vis spectra were characterized by an UV-vis spectrophotometer (UV, Cary 50, Varian, Hong Kong). Transmission electron microscope (TEM, Tecnai-12 Bio-Twin, FEI, Netherlands) and scanning electron microscope (SEM, S-3400N, Hitachi, Japan) were performed to observe the nanoparticle morphology. Confocal laser scanning microscopy (CLSM, TI2-E +A1 R, Nikon, Japan) and digital microscope (CKX53, Olympus, Japan) were used to observe morphology of microneedles.

The size distribution and zeta potential were determined by dynamic light scattering (DLS, ZS90, Malvern, UK). Flow cytometer (FCM, LSRFortessa, BD, USA) was performed to quantitatively analyze the immune cell phenotype.

## Synthesis of HSA NP and HSA NP Loading MTX (HM)

HSA was dissolved in distilled water with the concentration of 5 mg/mL, followed by the mixture with 2 mL MES (0.1 μmol·$L^{-1}$, pH = 5.2), 60 μL SDS (6%) and 50 μL (1%) $H_2O_2$. The reaction was under 65 °C for around 2 min. Until the solution turned into opalescent, predicting the formation of nanoparticles, the reaction was terminated. Afterwards, the solution was dialyzed in distilled water by a bag (10 kDa) for 24 h to remove MES, SDS and $H_2O_2$. The collected HSA NP was measured by DLS to determine the size and zeta potential.

For loading MTX, 1 mg of MTX was dissolved in 50 μL DMSO and mixed with a 5 mg/mL HSA solution. The subsequent steps were the same as described above. Ultimately, the reaction was terminated by dialysis using a 10 kDa bag. The size and zeta potential of HM was measured by DLS.

## Ultraviolet (UV) Detection

HM, MTX and HSA NP were detected by UV spectrophotometry to determine the amount of MTX loaded into the HSA NP. Also, different concentrations of MTX were prepared and measured by UV spectrophotometry to determine the loading content of MTX. Additionally, the loading capacity and loading efficiency of MTX in HM were determined by completely extracting the MTX after treating the HM with 2 mL of DMSO/ethanol (9:1, v/v), followed by sonication for 5 min. The MTX concentration of the different samples was measured by UV spectrophotometry, which had a characteristic absorption peak at 302 nm in the UV-visible (UV-vis) spectral region.

## In vitro Release and Stability Evaluation

HM dispersed in PBS was placed in a dialysis bag and further putted in 50 mL PBS (pH 7.4, 10×) in a shaking bed at 37 °C. At designated intervals, the samples were collected and analyzed to investigate the kinetic release behaviour of MTX.

Besides, HM was suspended in RPMI 1640 containing 10% FBS and the size was measured at days 1, 2, 3, 4 and 5 by DLS.

## Fabrication of MN and HM Microneedles Patch (HM/MN)

The stainless-steel MN mold (15×15 array, 600 μm height, 200 μm width at base, 500 μm interspacing) was obtained from Micropoint Technologies Pte Ltd. (Singapore). The mixture of degassed polydimethylsiloxane (PDMS) solution (prepolymer: curing agent=10:1, w/w) was added into the above-mentioned stainless steel MN template and cured in an oven at 90 °C for 1 h. The PDMS negative mold was obtained by carefully peeling off the master structure. Afterwards, 1 g of HA was dissolved in 1 mL deionized water. The above solution was casted into the PDMS mold and centrifuged at 4500 rpm for 5 min to fill up the cavities of the mold.

To construct the HM/MN patch, a mixture of 40 mg of HM and 0.5 g of HA was dissolved in 1 mL of water. Then, 40 μL of the mixed solution was added to the mold and centrifuged at 4500 rpm for 5 minutes. The excess solution was removed and 1 g/mL of HA was dispensed onto the mold to form the base layer. After drying in the desiccator, the HM/MN patches were obtained. Subsequently, the morphology of the MN patch was examined by SEM and digital microscopy.

## Mechanical Properties, Skin Penetration Ability and Dissolution Time of the MN

The mechanical properties of MN were measured using a UTM2502 electronic universal testing machine (Shenzhen Suns Technology Co., Ltd., Shenzhen, China). The compression force and distance were continuously recorded.

The skin penetration ability of MN was determined after isolating the back skin of mice, trimming it to a suitable thickness, and using it as a skin model. The MN loaded with 0.5% (w/v) methylene blue was pressed on the skin. After removing the base, the skin at the site where the MN punctured the skin was observed.

The MN patch was inserted into the exposed skin of C57BL/6 mice. At the designated time points (5, 10, 20, 30, 60, 90, 120, 180, and 300 s), the MN patch was removed and examined under a digital microscope to observe the dissolution of MN.

## In vivo LNs Targeting

C57BL/6 mice were used to investigate the targeting of HM/MN to LNs. First, the hair on the back of the mice was shaved off. Also, HSA NP was prelabeled with FITC, followed by loading into the MN patch. After transdermal administration with the developed HM/MN patch, the mice were sacrificed at the designated time points (4 and 10 h) and the LNs were removed to detect the fluorescence signal using a PerkinElmer IVIS® Spectrum In vivo Imaging System (PerkinElmer Inc., Waltham, MA, USA).

## In vivo Therapeutic Effect on Psoriatic Skin Lesions

A mouse model of psoriasis was developed by smearing imiquimod (IMQ) on the back of the mice. C57BL/6 mice were randomly divided into 4 groups and the hair on their back was shaved off in advance. On days 0, 2, and 4, IMQ was smeared on the back of the mice. On days 1, 3, and 5, the mice were correspondingly treated with Medical Vaseline, MTX, HM, and HM/MN patch (equivalent MTX, 15 μg/mouse). Normal mice treated with PBS were used as a control. On day 6, the mice were sacrificed to collect the back skin from 5 groups for hematoxylin and eosin (H&E) staining and cytokines (TNF-α and IL-6) detection. At the same time, the Psoriasis Area and Severity Index (PASI) score was used to assess the severity of psoriasis disease, evaluating the erythema, infiltration, and scaling. Each mouse was evaluated by three independent researchers every day. All the animal procedures were performed in accordance with the Guidelines for Care and Use of Laboratory Animals of Tongji University (Shanghai, China) and approved by the Animal Ethics Committee of Tongji University, School of Medicine (Shanghai, China).

## Immune Mechanism Investigation

Lymph nodes were also harvested to further make single-cell suspension. Then, the cell suspension was first blocked by CD16/32 for 30 min at 4 °C. After washing 3 times, cells were stained with Living/Dead dye and put at 4°C for 20 min. The cell suspension was washed as the same method and divided into two parts: one was stained with ACP-Cy7-CD45 and FITC-CD3 and another was stained with Qdot-605-CD11c for 30 min. Finally, cells were centrifuged and washed with PBS to analyze by a FCM.

# Results and Discussion

The schematic illustration of the synthesis of HM is outlined in Figure 1A. The HM/MN patch was constructed by the method of two-step casting described in previous reports (Figure 1B). On the IMQ induced mouse models of psoriasis, HM/MN is expected to efficiently deliver HM to the subcutaneous layer, which will subsequently accumulate in LNs and release MTX to suppress immune cells and inflammation (Figure 1C).

## Synthesis and Characterization of HM

The synthesized HSA NP with a hydrodynamic diameter of 68 nm are displayed in Figure 2A, and showed a spheroidal shape when observed by TEM as shown in Figure 2B. Further characterization of surface charge revealed that the zeta potential of HM decreased to around −20 mV compared with HSA NP, whose zeta potential was close to −15 mV (Figure 2C). The increased absolute value of the zeta potential indicated that HM had adequate stability, beneficial for storage and application. To further analyze the successful loading of MTX into HSA NP, UV spectrophotometry detection was performed. The results in Figure 2D reveal that MTX had two characteristic absorption peaks, one at 300 nm and the other at 400 nm. Meanwhile, HM showed a similar peak as MTX at 400 nm and another as HSA at 280 nm, an indication that MTX was loaded into HSA NP, which is consistent with a previous report.[23] The loading capacity and loading efficiency of MTX in HM were determined to reach 9.48 ± 1.04% and 92.1 ± 4.81%, respectively. The results in Figure 2E show that the size of HM remained unchanged for 5 days, which suggested that HM had good stability. The in vitro drug release profile of HM and HM/MN was evaluated in phosphate buffered saline (PBS) at neutral (pH 7.4). As shown in Figure 2F, MTX released from HM and HM/MN was similar and at a rate close to 60% within 48 h. The relatively slow-release speed could help the continuing anti-inflammation, suggesting the desired release profile.

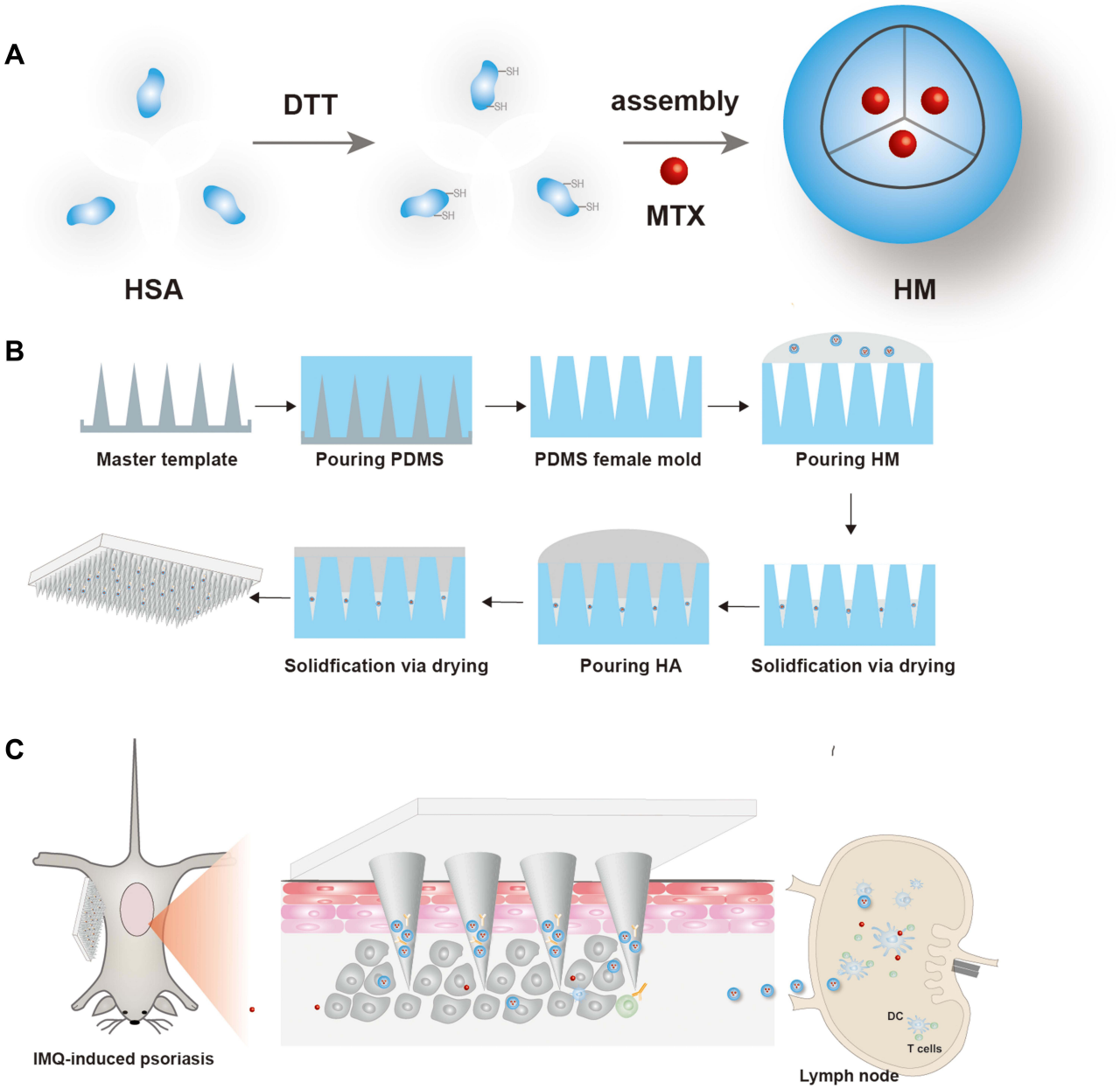


**Figure 1** Schematic image of (**A**) the main steps of synthesizing HM based on hydrophobic interactions between HSA and MTX molecules. (**B**) The fabrication of HM/MN via two-step casting and (**C**) delivery of HM/MN in psoriasis for efficient inhibition of dermatitis. After local administration, HM was delivered to subcutaneous tissue, which could further accumulate to LNs by the active targeting of HSA NP. MTX was released to inhibit the immune cells and trigger the inhibition of the secretion of pro-inflammatory cytokines, thus alleviating the progression of psoriasis.

## Construction and Evaluation of the HM/MN Patch

As shown in Figure 3A, the appearance of HA-based MN was observed by optical microscopy imaging (Figure 3D). The morphology was more directly examined by SEM imaging of HA-based MN (Figure 3C) and each needle appeared as a pyramid with an integrated needle tip, ensuring that MN could be successfully inserted into skin.[24] To mimic loading MN with HM, HSA NP labeled with FITC were loaded into MN, and observed by CLSM. The image displayed in Figure 3E shows that NP were mainly distributed in the needle tip and wall, which is favorable for the distribution of NP in the skin. The collected back skin tissues of mice were used to evaluate the ability of MN to pierce the skin tissue. Methylene blue was used to mimic drugs loaded into MN to investigate the intensity of MN-delivered drugs. As shown

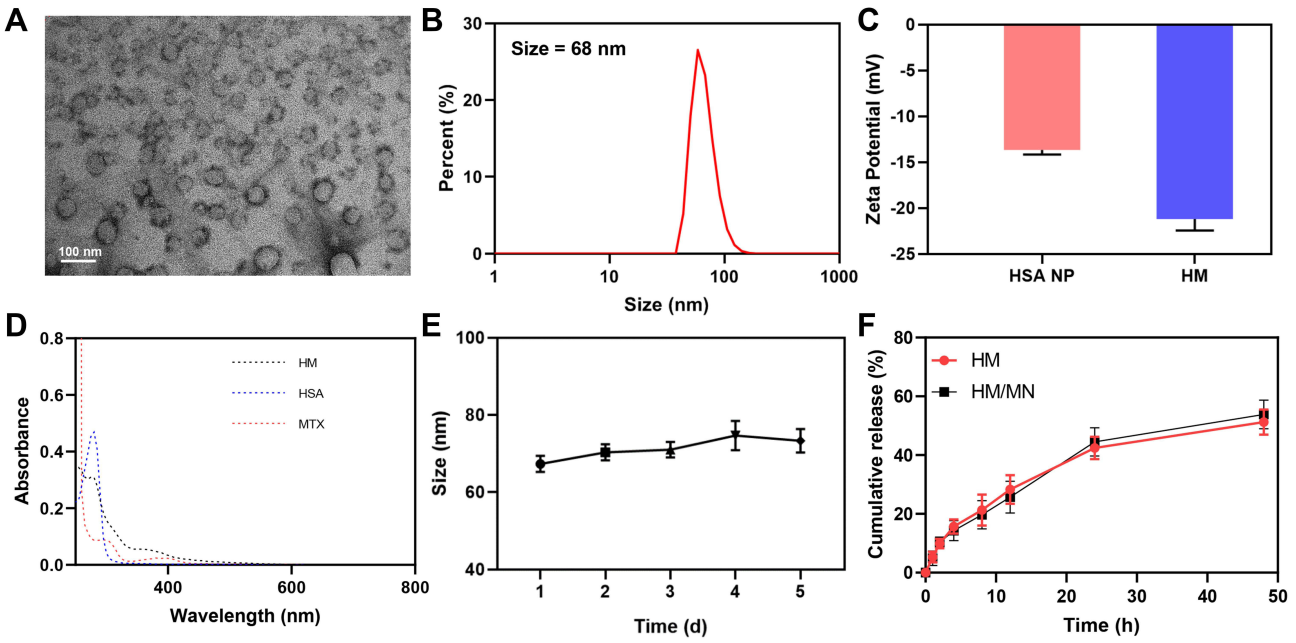


**Figure 2** (**A**) TEM and (**B**) the size distribution of HM. (**C**) Zeta potential of HSA NP and HM. (**D**) The UV absorbance of HSA NP, MTX and HM. (**E**) The stability of HM in RPMI 1640 medium containing 10% FBS within 5 days by determining the size. (**F**) MTX release from HM and HM/MN, dissolved in PBS (pH 7.4) within 48 h.

in Figure 3B, MN could readily pierce skin. The needle tip could quickly dissolve upon touching the intradermal interstitial fluid, thus releasing the drugs. It was also observed that a MN array was formed, indicating that all MN had successfully pierced the skin.[25] We also examined the mechanical strength of the MN patch. As shown in Figure 3F, the compressive force increased with the increase of compression displacement. There is no significant discontinuous point in the compressive force-compression displacement curve, indicating that the MN had undergone elastic deformation without obvious fracture.[26] The dissolution test revealed that the MN dissolved within 5 min, which is beneficial for HM release after administration.

## In vivo Therapeutic Effect on Psoriasis

The targeting effect of HSA NP on LNs was demonstrated by assessing the fluorescence intensity in LNs. As shown in Figure S1, LNs showed strong fluorescence intensity, indicating that the HSA NP had accumulated in the LNs. IMQ-induced psoriasis mouse model was used to evaluate the therapeutic outcome of psoriatic mice treated with the HM/MN patch. As shown in Figure 4A, the mouse model was successfully established by repeated administration of IMQ. Mice were randomly divided into 4 groups (n = 5), locally treated with Medical Vaseline, MTX, HM, and HM/MN patch, respectively. Representative images of mouse skin on day 6 are displayed in Figure 4B. The skin of the back of the mice in the model group exhibited typical erythema lesions, thickening, and peeling, suggesting the production of dermatitis after the application of IMQ.[27] In contrast, the damage was slightly improved by the administration of HM and MTX. It is notable that the HM/MN patch achieves the most successful therapeutic outcome. Further analysis of skin lesions by H&E staining, the thickness of the skin treated with IMQ increased significantly to around 80 μm. However, MTX, HM, and the HM/MN patch exhibited inhibitory effect on a skin lesion, with a thickness of 39.58±3.61, 33.75±2.16, 18.75 ±1.25 μm, respectively (Figure 4C and D). The minimum thickness of the skin in the group treated with the HM/MN patch indicated the excellent penetration achieved by using MN.[28] In addition, it is worth noting that a higher therapeutic effect was produced by HM than with free MTX, suggesting the targeting led to accumulation of HM in LNs. The evaluation of the progression and severity of psoriasis using the PASI scores of the mice on day 5 were revealed that the control group maintained the PASI score at 0.500 ± 0.866. In contrast, the IMQ-induced mouse model group exhibited the highest score at 9.833 ± 0.287, indicating the occurrence of the most severe skin lesions. After various treatments with MTX, HM and HM/MN patch, the PASI scores decreased to scores of 6.167 ± 0.289, 5.167 ±

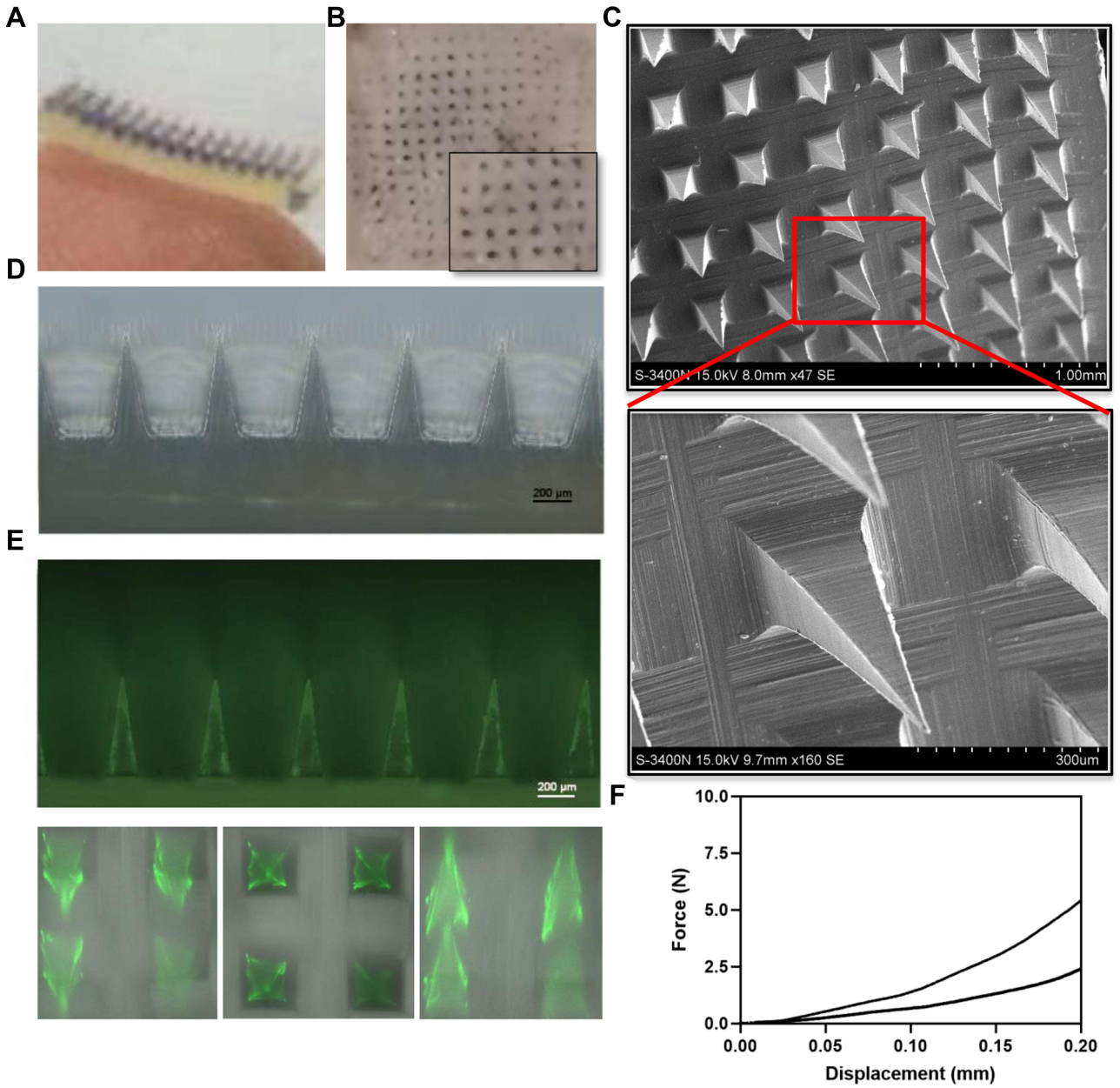


**Figure 3** (**A**) The external image of methylene blue-loaded MN. (**B**) Bright-field micrograph of neonatal mouse skin after the insertion by methylene blue-loaded MN in vitro. (**C**) The morphology of MN observed by SEM and (**D**) optical microscope. (**E**) HSA NP labeled by FITC loaded into MN imaged by CLSM. (**F**) The force displacement curves.

0.289 and 2.417 ± 0.144, respectively (Figure 4E). Importantly, treatment with the HM/MN patch clearly improved the psoriasis and exhibited a four-fold decrease in the PASI score compared with the model group. To assess the systemic impacts and safety of the different treatments, the weight of the mice was recorded and the pathology of major organs was examined. The analysis revealed that between the periods of day 0 to 6, the weight of mice with various treatments was maintained almost unchanged, although mice in the psoriasis model group showed a slight decrease in body weight (Figure 4F).

## Immune Mechanism Investigation

To the antipsoriatic mechanism, LNs were removed and used to prepare suspensions to analyze the subtypes of immune cells. The percent of $CD3^{+}CD45^{+}$ cells and $CD11c^{+}$ cells increased with the IMQ treatment, suggesting that the number

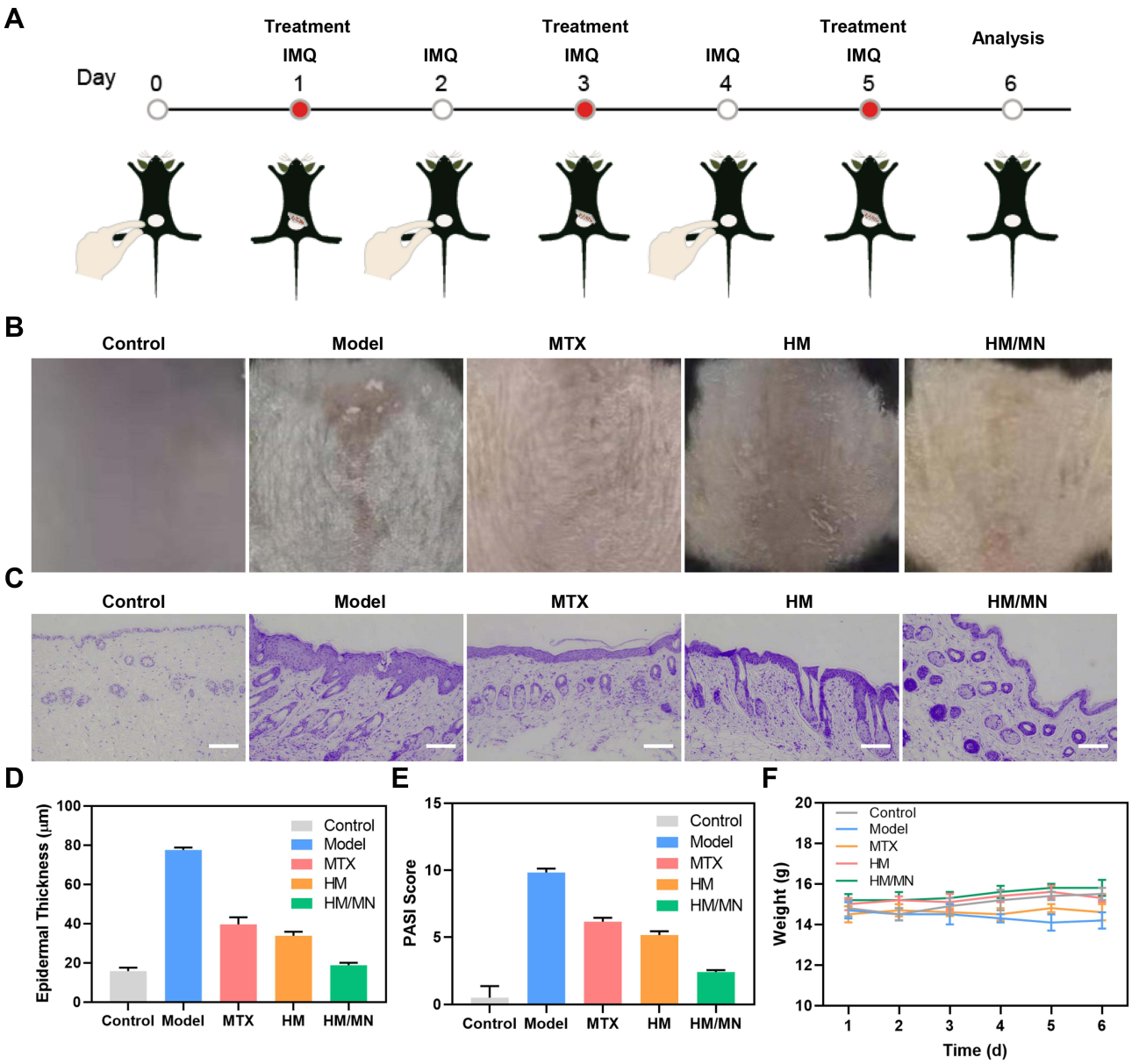


**Figure 4** Therapeutic treatments of free MTX, HM and HM/NM. (**A**) Experimental outline: psoriasis was induced by IMQ on days 1, 2, 3, 4 and 5, respectively. Mice received local treatment of MTX, HM and HM/MN on day 1, 3, 5. Five mice were used for each group. Representative photographs of (**B**) back skin of mice on day 6. (**C**) H&E staining images of skins (scale bar = 100 μm). (**D**) Evaluation of epidermal thickness and (**E**) statistical PASI score with different treatments. (**F**) Mice weight changes curve within 6 days.

of DC and T cells was significantly promoted, due to the skin lesion formation (Figure 5A–D). On the other hand, the percentage of DC and T cells in the group treated with MTX and HM decreased. Among these groups, the HM/MN treated mice had the lowest percent of DC and T cells, which showed the best therapeutic effect on psoriasis. The reduced number of DC and T cells in LNs of mice treated with HM compared with those treated with free MTX indicated that the accumulation of HM in LNs can suppress immune cells to achieve an enhanced antipsoriatic therapeutic effect. In addition, the relative levels of cytokines in skin tissues were measured in the appropriate suspensions prepared with the corresponding ground tissues. The local effect of the HM/MN patch on the levels of IL-6 and TNF-α was also evaluated due to their critical role in the pathogenesis of psoriasis. IL-6 and TNF-α were found to be strongly enhanced in IMQ-treated mouse skin. Remarkably, the various treatments were shown to downregulate the IL-6 and TNF-α levels, thereby inhibiting the epidermal proliferation, and attenuating psoriasis-like dermatitis (Figure 5E and F). Moreover, when

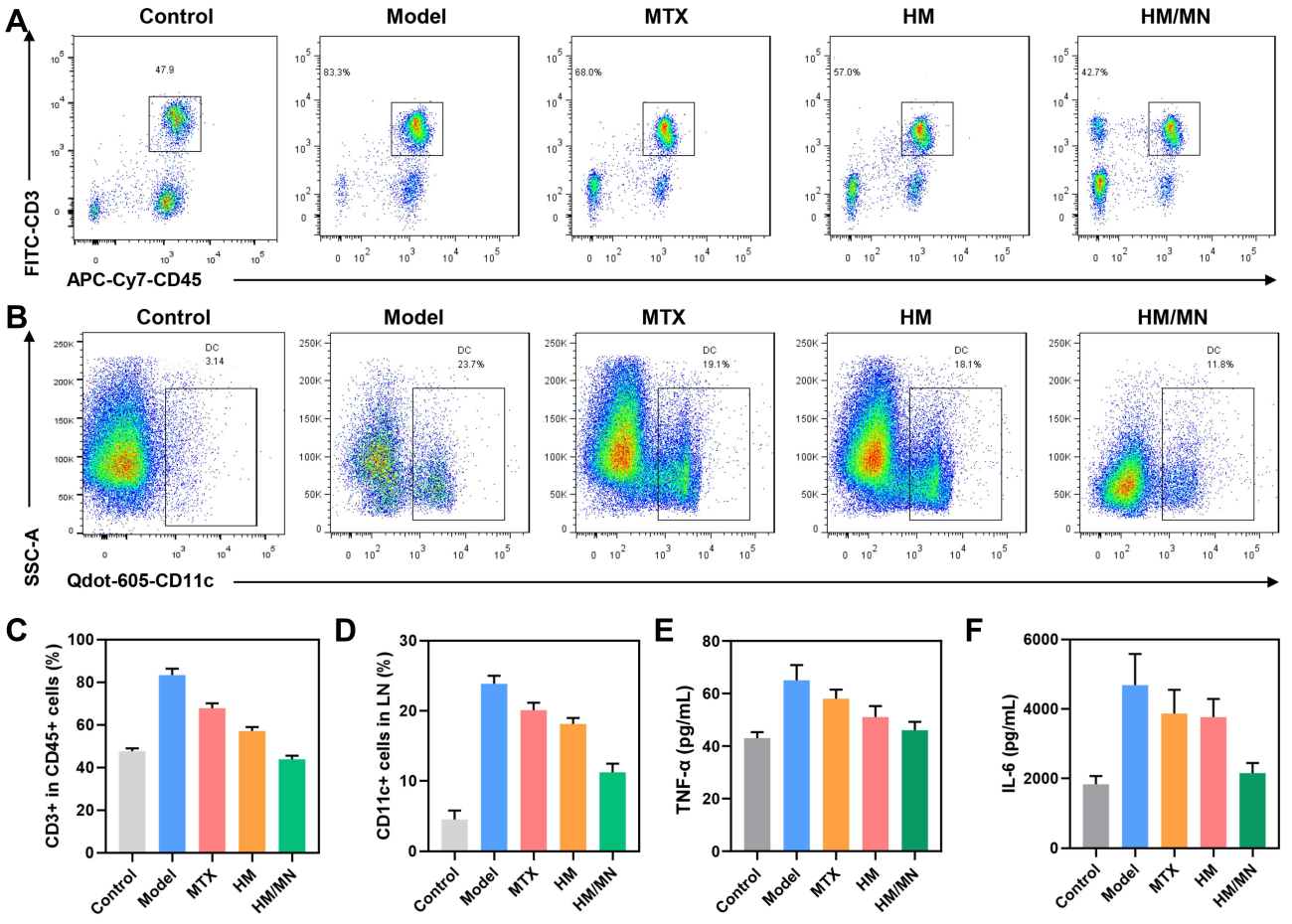


**Figure 5** Representative flow images of (**A**) $CD3^+$ cells gating on $CD45^+$ cells and (**B**) $CD11c^+$ cells in LN. (**C**) Statistical evaluation of $CD3^+$ in $CD45^+$ cells and (**D**) $CD11c^+$ cells in LN. Cytokines level of (**E**) TNF-α and e) IL-6 in skin after various treatments at day 6.

treated with the HM/MN patch, the expression levels of TNF-α and IL-6 were decreased to levels close to those in the normal group. These significantly reduced cytokine levels implied that the HM/MN was protective against IMQ-induced inflammatory injury in mice.

## H&E Staining Analysis

The histopathological studies performed on the collected major organs (Figure 6) showed no obvious inflammation or injury in any of the mice in the treatment groups, further indicating that the treatment with the HM/MN patch did not produce any appreciably adverse effects. Together, these results demonstrate that MN showed both excellent efficacy and a robust safety profile in the treatment of psoriasis.

# Conclusions

In this study, we describe the development of a HA-based dissolvable MN patch to deliver HSA NP loaded with MTX for the treatment of psoriasis. We successfully synthesized HM, which were shown to have a spheroidal shape with the desired MTX release profile. The developed HM/MN patch could pierce the skin, thus ensuring the successful subcutaneous delivery of the drug. This study also revealed that the HM/MN patch could attenuate epidermal hyperplasia, reduce the production of IL-6 and TNF-α, and ultimately improve psoriasis in the IMQ-induced mouse model of psoriasis. Moreover, compared to free MTX, HM showed an enhanced therapeutic effect with decreased number of DC cells and T cells in LNs, and also exhibited augmented targeting to LNs with the

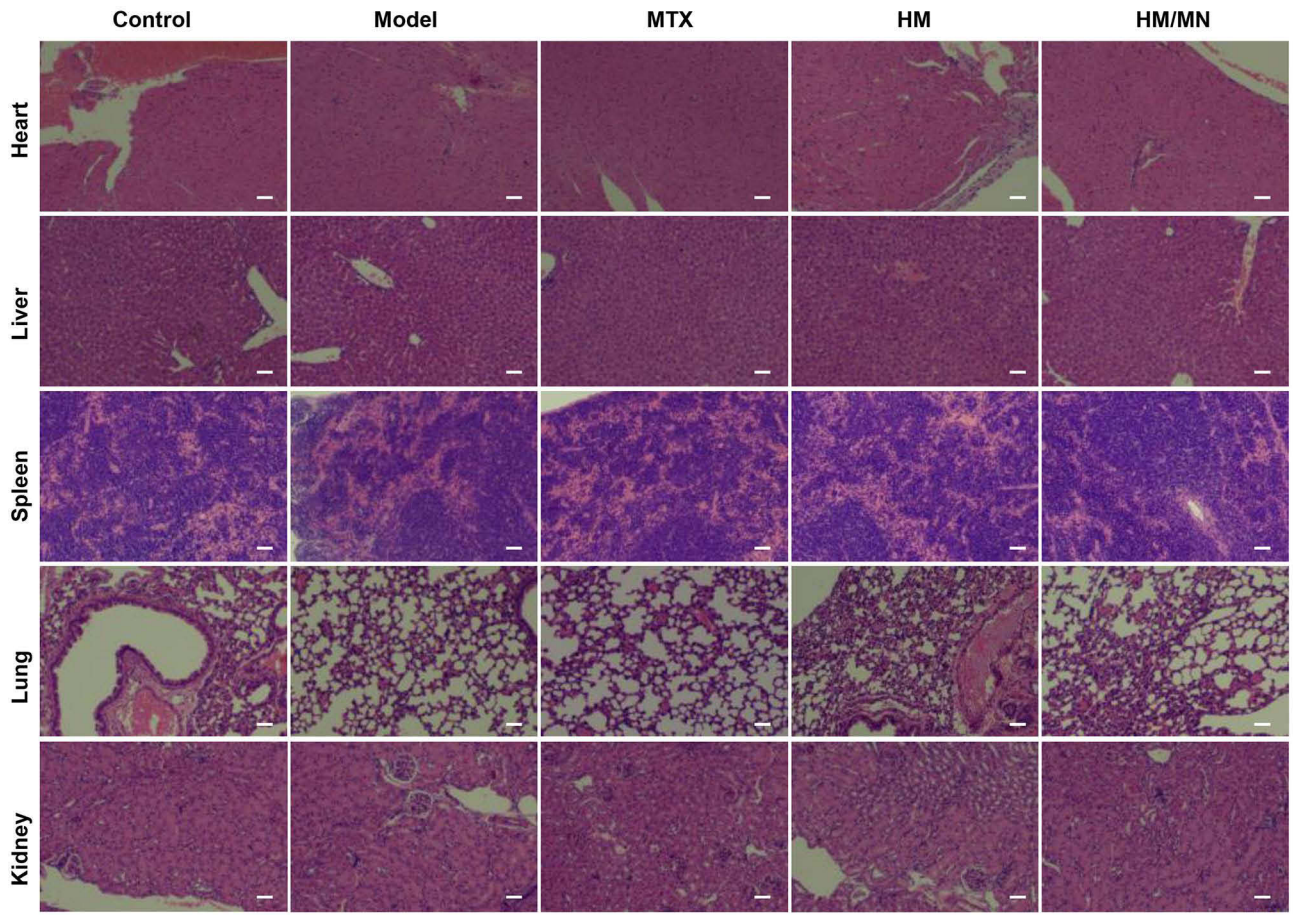


**Figure 6** H&E staining images of major organs including heart, liver, spleen, lung and kidney (scale bar = 50 μm).

assistance of NP. Taken together, our study provides an alternative antipsoriasis therapy based on a MN patch, which holds attractive potential for clinical translation.

## Acknowledgments

This work was supported by the National Natural Science Foundation of China (82071630, 81771560), the grants from the Clinical research project on health industry of Shanghai Health Committee (201940200) and sponsored by the Shanghai Sailing Program (21YF1435800).

## Disclosure

The authors declare no conflict of interest.

## References

1. Herster F, Bittner Z, Archer NK, et al. Neutrophil extracellular trap-associated RNA and LL37 enable self-amplifying inflammation in psoriasis. *Nat Commun*. 2020;11(1):105. doi:10.1038/s41467-019-13756-4
2. Griffiths CEM, Barker JNWN. Psoriasis 1 - Pathogenesis and clinical features of psoriasis. *Lancet*. 2007;370(9583):263–271. doi:10.1016/S0140-6736(07)61128-3
3. Vena GA, Cassano N, Iannone F. Update on subcutaneous methotrexate for inflammatory arthritis and psoriasis. *Ther Clin Risk Manag*. 2018;14:105–116. doi:10.2147/TCRM.S154745
4. Yelamos O, Puig L. Systemic methotrexate for the treatment of psoriasis. *Expert Rev Clin Immu*. 2015;11(5):553–563. doi:10.1586/1744666X.2015.1026894
5. Shetty A, Cho W, Alazawi W, Syn WK. Methotrexate hepatotoxicity and the impact of nonalcoholic fatty liver disease. *Am J Med Sci*. 2017;354(2):172–181. doi:10.1016/j.amjms.2017.03.014

6. Mielanczyk A, Mrowiec K, Kupczak M, et al. Synthesis and in vitro cytotoxicity evaluation of star-shaped polymethacrylic conjugates with methotrexate or Acitretin as potential antipsoriatic prodrugs. *Eur J Pharmacol*. 2020;866:172804. doi:10.1016/j.ejphar.2019.172804
7. Ramadon D, McCrudden MTC, Courtenay AJ, Donnelly RF. Enhancement strategies for transdermal drug delivery systems: current trends and applications. *Drug Deliv Transl Re*. 2022;12(4):758–791. doi:10.1007/s13346-021-00909-6
8. Lee H, Song C, Baik S, Kim D, Hyeon T, Kim DH. Device-assisted transdermal drug delivery. *Adv Drug Deliver Rev*. 2018;127:35–45. doi:10.1016/j.addr.2017.08.009
9. Neupane R, Boddu SHS, Renukuntla J, Babu RJ, Tiwari AK. Alternatives to biological skin in permeation studies: current trends and possibilities. *Pharmaceutics*. 2020;12(2):152. doi:10.3390/pharmaceutics12020152
10. Xu JM, Chen H, Chu ZY, et al. A multifunctional composite hydrogel as an intrinsic and extrinsic coregulator for enhanced therapeutic efficacy for psoriasis. *J Nanobiotechnol*. 2022;20(1):155. doi:10.1186/s12951-022-01368-y
11. Jeong WY, Kwon M, Choi HE, Kim KS. Recent advances in transdermal drug delivery systems: a review. *Biomater Res*. 2021;25(1):24. doi:10.1186/s40824-021-00226-6
12. Sabbagh F, Kim BS. Recent advances in polymeric transdermal drug delivery systems. *J Control Release*. 2022;341:132–146. doi:10.1016/j.jconrel.2021.11.025
13. Singh P, Carrier A, Chen YL, et al. Polymeric microneedles for controlled transdermal drug delivery. *J Control Release*. 2019;315:97–113. doi:10.1016/j.jconrel.2019.10.022
14. Yang J, Liu XL, Fu YZ, Song YJ. Recent advances of microneedles for biomedical applications: drug delivery and beyond. *Acta Pharmacol Sin B*. 2019;9(3):469–483. doi:10.1016/j.apsb.2019.03.007
15. Liu LB, Wang QQ, Liao HW, et al. Soluble microneedle patch with photothermal and NO-release properties for painless and precise treatment of ischemic perforator flaps. *J Material Chemistry B*. 2021;9(37):7725–7733. doi:10.1039/D1TB00491C
16. Zhu JY, Tang XD, Jia Y, Ho CT, Huang QR. Applications and delivery mechanisms of hyaluronic acid used for topical/transdermal delivery - A review. *Int J Pharmaceut*. 2020;578:119127. doi:10.1016/j.ijpharm.2020.119127
17. Wang C, Ye YQ, Hochu GM, Sadeghifar H, Gu Z. Enhanced cancer immunotherapy by microneedle patch-assisted delivery of Anti-PD1 antibody. *Nano Lett*. 2016;16(4):2334–2340. doi:10.1021/acs.nanolett.5b05030
18. Kirtane AR, Verma M, Karandikar P, Furin J, Langer R, Traverso G. Nanotechnology approaches for global infectious diseases. *Nat Nanotechnol*. 2021;16(4):369–384. doi:10.1038/s41565-021-00866-8
19. Delfi M, Sartorius R, Ashrafizadeh M, et al. Self-assembled peptide and protein nanostructures for anti-cancer therapy: targeted delivery, stimuli-responsive devices and immunotherapy. *Nano Today*. 2021;38:101119. doi:10.1016/j.nantod.2021.101119
20. Chen Q, Liang C, Wang X, He JK, Li YG, Liu Z. An albumin-based theranostic nano-agent for dual-modal imaging guided photothermal therapy to inhibit lymphatic metastasis of cancer post surgery. *Biomaterials*. 2014;35(34):9355–9362. doi:10.1016/j.biomaterials.2014.07.062
21. Bunschoten A, Buckle T, Kuil J, et al. Targeted non-covalent self-assembled nanoparticles based on human serum albumin. *Biomaterials*. 2012;33(3):867–875. doi:10.1016/j.biomaterials.2011.10.005
22. Sheng ZH, Hu DH, Zheng MB, et al. Smart human serum albumin-indocyanine green nanoparticles generated by programmed assembly for dual-modal imaging-guided cancer synergistic phototherapy. *ACS Nano*. 2014;8(12):12310–12322. doi:10.1021/nn5062386
23. Liu L, Hu FL, Wang H, et al. Secreted protein acidic and rich in cysteine mediated biomimetic delivery of methotrexate by albumin-based nanomedicines for rheumatoid arthritis therapy. *ACS Nano*. 2019;13(5):5036–5048. doi:10.1021/acsnano.9b01710
24. Chang H, Zheng MJ, Yu XJ, et al. Patch to rapidly extract skin interstitial fluid for timely metabolic analysis. *Adv Mater*. 2017;29(37):1702243. doi:10.1002/adma.201702243
25. Wang JQ, Ye YQ, Yu JC, et al. Core-shell microneedle gel for self-regulated insulin delivery. *ACS Nano*. 2018;12(3):2466–2473. doi:10.1021/acsnano.7b08152
26. Luo FQ, Chen GJ, Xu W, et al. Microneedle-array patch with pH-sensitive formulation for glucose-responsive insulin delivery. *Nano Res*. 2021;14(8):2689–2696. doi:10.1007/s12274-020-3273-z
27. Schwarz A, Philippsen R, Schwarz T. Induction of regulatory T cells and correction of cytokine disbalance by short-chain fatty acids: implications for psoriasis therapy. *J Invest Dermatol*. 2021;141(1):95. doi:10.1016/j.jid.2020.04.031
28. Du HY, Liu P, Zhu JJ, et al. Hyaluronic acid-based dissolving microneedle patch loaded with methotrexate for improved treatment of psoriasis. *ACS Appl Mater Interfaces*. 2019;11(46):43588–43598. doi:10.1021/acsami.9b15668